Geological Quarterly, 2019, **63** (4): 786–800
DOI: http://dx.doi.org/10.7306/gq.1508

CO_2 sorption properties of selected lithotypes of lignite from Polish deposits

Barbara BIELOWICZ[1, *] and Paweł BARAN[2]

[1] AGH University of Science and Technology, Faculty of Geology, Geophysics and Environment Protection, al. A. Mickiewicza 30, 30-059 Kraków, Poland

[2] AGH University of Science and Technology, Faculty of Energy and Fuels, al. A. Mickiewicza 30, 30-059 Kraków, Poland

Bielowicz, B., Baran, P., 2019. CO_2 sorption properties of selected lithotypes of lignite from Polish deposits. Geological Quarterly, **63** (4): 786–800, doi: 10.7306/gq.1508

Associate editor: Wojciech Drzewicki

Sorption studies, to determine the CO_2 sorption capacity of coal, were carried out using eight ortho-lignite samples of different lithotypes, to investigate the possibility of CO_2 storage in lignite deposits. Equations determining a number of parameters and indicators used to delineate the experimental data and to differentiate the samples examined include: Langmuir isotherms; the Dubinin-Radushkevich (DR) equation that describes the theory of volume filling of micropores; and the Brunauer, Emmett and Teller (BET) equation used to calculate the volume and surface area of a monolayer. The results obtained were compared with the petrographic composition and ultimate and proximate analysis of lignite. There is a large correlation between sorption and petrographic composition, a positive impact of the Gelification Index on the sorption process and a clear relationship between the sorption (Langmuir and DR) and ash content. The best CO_2 sorption properties were found for xylo-detritic and detro-xylitic lignites. Based on the tests carried out, a preliminary assessment of the suitability of lignite for CO_2 storage can be made.

Key words: sorption CO_2, lignite, Gelification Index, maceral composition.

INTRODUCTION

With increasing concern for the environment, new materials that can be used to eliminate harmful substances are being sought. The search for and analysis of new methods for the storage of gaseous and waste fuels can help to achieve this objective. Deep, undeveloped coal seams can potentially be used for the storage of CO_2 of anthropogenic origin. The carbon dioxide may be injected into coal seams, where it can be stored permanently, provided that the coal seams will be never mined. There is currently increased interest in the idea of CO_2 storage in coal seams combined with enhanced coal bed methane recovery (ECBM; Reznik et al., 1984; Gale and Freund, 2001; Mazzotti et al., 2009; Harpalani and Mitra, 2010; Li and Fang, 2014; Perera and Ranjith, 2015; Kudasik et al., 2017; Pan et al., 2018).

Studies of this type are being conducted worldwide, mainly in the USA (e.g., the ARC ECBM Recovery Project, Coal-seq), India, China, and Europe (CO_2 storage in the Upper Silesian Coal Basin in Poland, RECOPOL project). Due to the nature of the process itself and associated safety issues, a seam used for the storage of carbon dioxide has to meet a number of criteria.

The characteristic properties of lignite, mainly the well-developed porosity and chemical nature of the specific surface, allow one to deploy it as a potential precursor for the preparation of microporous adsorbents. On account of the possibility of changing its structure, ranging from one of low porosity to one of strictly microporous character and of surface modification by fragmentation into fine grained coal, there are numerous applications for lignite e.g. purification of soils from heavy metals (Karczewska et al., 1996).

Polish lignites range in age from Triassic to Paleogene (Paleocene, Eocene and Oligocene) and Neogene (Miocene and Pliocene). In the Paleogene and Neogene formations in Poland, 10 groups of coal seams are found, of which nationally only three (the first Mid-Polish lignite seam, the second Lusatian lignite seam and the third Ścinawa lignite seam) and locally five (additionally, the Lubin IIA lignite seam and the fourth Dąbrowa lignite seam) are of economic importance. Lignite from Paleogene and Neogene formations, most commonly found in Poland, are of the greatest economic significance. The largest lignite deposits in Poland were developed in the Miocene. The deposits were formed under conditions of light pressure, slightly elevated temperature and under an overburden with a thickness from 30 to 300 m. The thickness of the lignite deposits ranges from several to several tens of metres; they may also occur in the form of lenses. The total resources are estimated to be 23,516.19 million tons according to the United

* Corresponding author, e-mail: bbiel@agh.edu.pl

Received: February 9, 2019; accepted: September 17, 2019; first published online: December 31, 2019

Nations Framework Classification of Resources (UNFC). As of December 31, 2016, 91 lignite deposits were explored in Poland, of which 74 were documented and are still undeveloped. Polish extractable lignite resources amount to 1,129.06 million tons, which is ~0.8% of the global reserves of this type (PGI-NRI, 2017). Lignite deposits whose exploitation is not economically viable can be used for CO_2 sequestration. Attention is therefore focused on deep lignite deposits and seam thickness, the exploitation of which is not economically feasible. At the same time, the deposits discussed are insulated deposits; thus, the prevailing geological conditions could enable carbon capture and storage. The geological and depositional conditions required for CO_2 storage are generally similar to the requirements for UCG, e.g. the depth of the deposit, thickness and nature (low-permeability, structurally coherent and laterally continuous) of insulating layers, presence of groundwater reservoirs and the lack of tectonic disturbances in the direct exploitation zone. Studies performed on the possibility of underground gasification in Poland have shown that the deposits at Ścinawa–Głogów, Gostyń, Krzywiń, Węglewice and Kamieńsk can be potentially used for CO_2 storage (Bielowicz and Kasiński, 2014). Generally, the limited access to samples from these lignite deposits prevents sorption studies. Therefore, it is crucial to determine trends allowing a preliminary assessment of the suitability of coal for CO_2 storage based on the available archival data, including petrographic composition and proximate and ultimate analysis. In addition, CO_2 sorption studies are important from the point of view of coal structure analysis. Low-temperature nitrogen adsorption, widely used for adsorbent structure analysis, does not give satisfactory results in the case of coal (both bituminous coal and lignite) due to the very slow rate of the activated diffusion. The relatively high value of the critical temperature of carbon dioxide (304.5 K) is the reason why adsorption measurements at room temperature are justified due to the high rate of activated if fusion. This is supported by the results of low-angle XRD analysis of surfaces (Grimes, 1982).The present study investigated the sorption properties of lignite from four Polish deposits: Jóźwin, Sieniawa, Bełchatów and Turów. Samples of the various lignite lithotypes were collected. Measurements of CO_2 sorption isotherms under elevated pressures were carried out. A formal mathematical description of the isotherms obtained, based on the Langmuir, Dubinin-Radushkevich and Brunauer, Emmett and Teller (BET) equations, was developed. The relationships between coal quality, maceral composition and sorption properties were also investigated.

The sorption properties of lignite have been examined by many authors including Azmi et al. (2006), Botnen et al. (2009), Gensterblum et al. (2010) and Zelenka and Taraba (2014). In Poland, sorption characteristics have also analysed (Baran et al., 2010, 2014, 2013; Macuda et al., 2011). The impact of petrographic composition on the CO_2 sorption in low-rank coals has not been widely studied. Most of the previous studies have focused on bituminous coal and methane sorption (Lamberson et al., 1991; Clarkson and Bustin, 1997; Crosdale et al., 1998; Laxminarayana and Crosdale, 1999; Mastalerz et al., 2004).

RESEARCH METHODOLOGY

The study used eight lignite samples from Polish deposits, namely: the Jóźwin deposit (three samples), the Turów deposit (two samples), the Sieniawa deposit (two samples) and the Bełchatów deposit (one sample). Samples of various lignite lithotypes such as detritic, detro-xylitic and xylitic lignite were collected.

The samples were air-dried for one week to reach air-dry equilibrium. It is well-known that moisture has a significant impact on the sorption capacity of coal (Wang et al., 2011; Švábová et al., 2012). Therefore, in order to avoid oxidation of the surface, which in the case of carbon dioxide could affect its sorption capacity due to the presence of a quadrupole moment in the molecule, the samples were not dried at elevated temperatures, but in the open air.

The samples were ground to a size of <1 mm and used as material for polished sections (polished pellets), which were prepared according to the ISO 7404-2:2009 standard. Petrographic examination to determine maceral group composition was carried out in both reflected white and blue light with the use of a *Zeiss Opton* microscope and in accordance with the ISO 7404-3:2009 standard. The maceral composition of lignite was determined according to ICCP guidelines (ICCP, 2001a, b; Sýkorová et al., 2005; Pickel et al., 2017). Macerals from the liptinite group were examined under fluorescent light. The maceral nomenclature for the liptinite group was applied according to Pickel et al. (2017). The average random reflectance of ulminite B was determined under standard conditions, i.e. in monochromatic light with a wavelength of 546 nm and immersion oil (n = 1.518), using a *Zeiss MPM-400* photometer equipped with a MSP-20 system processor. Random reflectance measurements in ortho-lignite were carried out on the surface of ulminite B (Sýkorová et al., 2005). The maceral group content analyses were carried out at 500 equally spaced points on the polished pellet surfaces. Tissue Preservation Index (*TPI*) and Gelification Index (*GI*) were determined based on the equation of Diessel (1986) modified according to the guidelines of Kalaitzidis et al. (2004):

- *GI* = (ulminite+humocollinite+densinite)/(textinite+attrinite+inertinite);
- *TPI* = (humotelinite+corpohuminite+fusinite)/(attrinite+densinite+gelinite+inertodetrinite).

Proximate and ultimate analyses were carried out for both coal and ash according to ISO standards. The samples were ground to a size of 0.2 mm. Proximate analysis covered: moisture content, ash content, volatile matter content and the gross calorific value determination. Ultimate analysis included carbon, hydrogen, nitrogen and sulphur content determination using a Leco analyzer. The chemical composition of coal was analysed by ICP-OES/MS at the Bureau Veritas Minerals Laboratory. ICP-MS analysis was performed on a 15 g sample after modified aqua regia digestion (1:1:1 HNO_3:HCl:H_2O) for low to ultra-low determination of both coal and ash.

The examination of the porous texture of the coal samples examined was carried out at the AGH University of Science and Technology (Faculty of Energy and Fuels), using *Pascal 140 CE* and *Pascal 440* porosimeters. The porosimeters (140-low pressure and 440-high pressure) work in the pressure range from 0.3 kPa up to 150.0 MPa, which enables the measurement of pore radii from ~7500 nm to 2 nm. The apparatus registers the volume of mercury penetrating the pores of the material examined, showing the dependence curves of open pore volume and pore volume distribution on the pressure applied and radii, respectively. Pore radii corresponding to the specified pressure values are calculated based on the Washburn equation. Taking into account the large spread of the parameters, the results are presented using a logarithmic number system. Sorption tests were performed using a volumetric apparatus (Fig. 1).

Details of carrying out the measurements and determining sorption capacity can be found in Baran and Zarębska (2015).

The criterion for achieving thermodynamic equilibrium was to achieve a constant gas pressure in the ampoule. The next isothermal point was obtained by dosing the subsequent amount of gas.

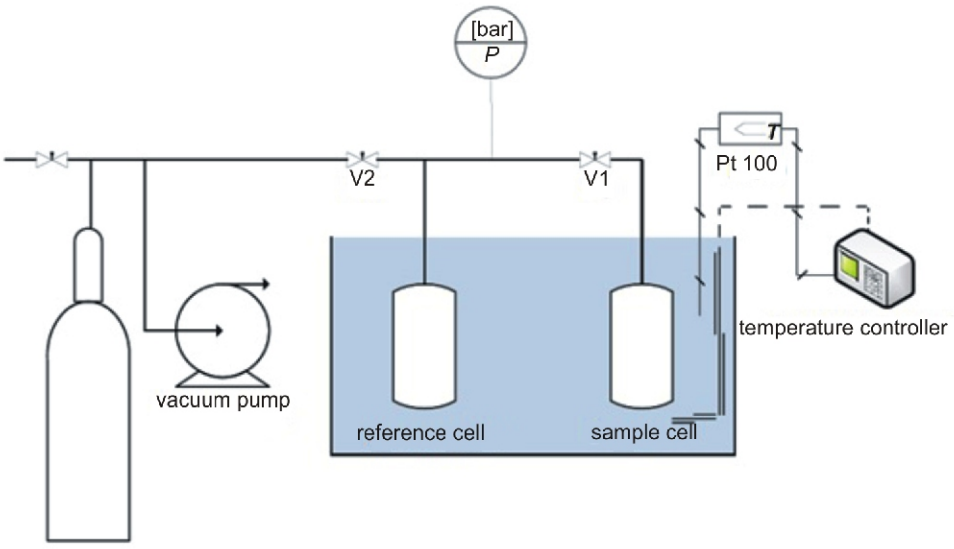

Fig. 1. The test equipment for measuring sorption isotherms – a schematic diagram

The adsorbed volume was calculated from the pressure difference before and after the sorption process, taking into account the dead volume of the apparatus (determined by subtracting the volume of coal grains from the total volume of the apparatus). The volume of gas contained in the coal mass unit was converted into standard conditions: p = 0.1 MPa, T = 298.2 K), at a given pressure and the temperature measured inside the ampoule. The exact procedure of calculating the sorption capacity can be found in Baran et al. (2014).

Carbon dioxide sorption isotherms for each sample examined were measured at 298 K. Before the measurements, the samples were degassed for 24 hours. The criterion of sorption equilibrium is fulfilled on the condition that the time-constant gas pressure in the ampoule is reached for ~24 hours. The next point of the isotherm was obtained by dosing the subsequent portion of gas. In the case of CO_2, a divergence from ideal gas properties shall be taken into account. The calculations were carried out using the Span-Wagner equation of state (Span and Wagner, 1996).

The experimental results were described using three models of sorption isotherms: Langmuir: (1 – Langmuir, 1918), BET (2 – Brunauer et al., 1938) and Dubinin–Radushkevich (3 – Dubinin, 1960) in the following forms:

$$\frac{{}_{m\,L}\;K_L\;\frac{p}{p_s}}{1\;K_L\;\frac{p}{p_s}} \qquad [1]$$

$$\frac{{}_{m\;BET}\;\;C\;\;\frac{p}{p_s}}{1\;\frac{p}{p_s}\;\;1\;\;C\;\;1\;\;\frac{p}{p_s}} \qquad [2]$$

$$V\;\;V_0 e^{\;\frac{RT}{E_0}\ln\frac{p_s}{p}\;\;^2} \qquad [3]$$

where: $_{m(L)}$ and $_{m(BET)}$ – the capacity of the Langmuir and BET sorption monolayers [cm^{3}g^{-1}]; K_L – the constant of the Langmuir equation; C – the constant of the BET equation; V_0 – the total micropore volume [cm^{3}g^{-1}]; p_s – saturated vapor pressure [hPa]; E_0 – characteristics of the energy of sorption for standard vapor [kJ/mol]; – the coefficient of similarity (convergence) of a sorbate.

The constants of Langmuir, BET and DR equations were calculated by fitting the linear forms of isotherms to the experimental data. Linear isotherms can be represented by the following equations:

$$\frac{\frac{p}{p_s}}{\;\;\frac{1}{K_L\;\;_{m\;BET}}\;\;\frac{1}{_{m\;BET}}\;\;\frac{p}{p_s}} \qquad [4]$$

$$\frac{\frac{p}{p_0}}{1\;\;\frac{p}{p_s}}\;\;\frac{1}{_{m\;BET}}\;\;\frac{C\;\;1}{_{m\;BET}\;\;C}\;\;\frac{p}{p_s} \qquad [5]$$

$$\ln V\;\;\ln V_0\;\;\left(\frac{RT}{E_0}\right)^2\ln^2\frac{p}{p_s} \qquad [6]$$

Correlation and regression analyses were used to determine correlations between the different parameters. Pearson's linear correlation coefficients (r) were calculated. The significance of correlation coefficients has been assessed and analysed. The test of statistical significance has been performed using the Student's t distribution. When calculating the regression equation, the least squares sum method was used. Finally, the reverse regression was performed. In addition, the inverse regression and residual standard error were calculated and the estimation of regression coefficients was carried out in order to determine the confidence interval for regression, Neyman intervals and the regression prediction error. Correlation coefficient values were characterized based on Table 1.

Table 1

The interpretation of correlation coefficient values

Value of *r*	Interpretation
(0.00–0.20)	slight, almost negligible relationship,
<0.20–0.40)	low correlation; definite but poor relationship
<0.40–0.70)	moderate correlation; substantial relationship
<0.70–0.90)	high correlation; marked relationship
<0.90–1.00)	very high correlation; very dependable relationship

GEOLOGY OF THE DEPOSITS STUDIED

The Turów deposit, located in the Zittau Basin (Niecka Żytawska), formed during orogenic subsidence. The Neogene and Paleogene formations are ~350 metres thick and contain three lignite seams (Fig. 2). Based on palynological analysis, the lower seam was determined to be of Lower Miocene age, which allows correlation with the third Ścinawa lignite seam (Piwocki and Ziembińska-Tworzydło, 1997). Its thickness ranges from 20 to 30 metres. The upper seam reaches 42 m in the central part of the southern area and extends towards the edge of the basin. It is estimated to be of Lower Miocene – lowest Middle Miocene age, which correlates with the second Lusatia lignite seam. Channel samples of lignite for the detailed analysis were collected from the exploitation walls in the eastern part of the deposit according to the ISO 13909-1:2016 standard.

The Jóźwin deposit is located in the northeastern part of the Mogilno–Łódź Synclinorium (Fig. 2). It has the form of a wide lens and is classified as a platform-type deposit (stratoidal type).The lignite-bearing succession is mainly composed of Neogene deposits (Middle Miocene) underlain by weathered marls of Paleocene age and overlain by Pleistocene deposits. The main part of the lignite deposits is the lignite succession located in the lower part of the Poznań Formation and within the first Mid-Polish lignite seam, also referred to as the Konin seam (Sadowska and Giża, 1991). The thickness of the coal seam ranges from 0.2 to 30 m. The seam disappears in tunnel valleys. Green clays, sands and red clays of the Poznań Formation (Piwocki, 2004) and Pleistocene and Holocene deposits characterized by highly variable lithology and facies development can be found locally in the roof of the deposit.

The Sieniawa deposit (Fig. 2) is located in the northern part of the Lubuska Upland. It is the smallest and the longest (since 1873) exploited deposit in Poland. It is a platform-type deposit (glaciotectonic type). As a result of glaciotectonic folding of the Paleogene and Neogene deposits, 27 anticlines are developed within the second Lusatian lignite seam deposits. Currently, the Sieniawa deposit is a private (commercial) opencast mine, conducting mining activities in the IX anticline. The lignite-bearing formation is the Ścinawa Formation, including a single second Lusatian lignite seam with a thickness in the range from 6 to 18 m. In glaciotectonically disturbed zones, the thickness of the lignite-bearing formation increases up to 30 m (Bielowicz and Kasiński, 2014). The accompanying seams (1–5) are located locally at the floor of the main deposit and have a thickness in the range from 0.3 up to 3 m. They are overlain by the Pawłowice Formation composed of sand and mudstones (Szwed-Lorenz, 1991).

The Bełchatów deposit (Fig. 2) is located in the southern part of the Middle Polish synclinorium, within the Kleszczów graben. The Bełchatów and Szczerców deposits are separated by up domed Zechstein rocks related to the “Dębina” salt dome. The deposit discussed is cratonic, of tectonic (graben) type. The thickness of Neogene deposits ranges from 150 to 400 m and comprise successions of lignite, lignite, clay and lignite and sand-clay, overlain by a continuous cover of Pleistocene deposits with a thickness from a few to >100 m. In the profile, there are one or two lignite seams containing four thin sub-seams including deposits of Lower and Middle Miocene age. According to the marine stratigraphic scheme of the Paratethys area, the one or two lignite seams correspond to the Ottnang, Carpathian and the Lower Badenian. In the lithostratigraphic scheme of the Polish Lowlands, the thin lignite sub-seams noted correspond to the third Ścinawa, the second Lusatian and the first Mid-Polish lignite seams. The second Lusatia and third Ścinawa seams, often occurring together (as a lignite succession), are of the greatest economic importance. Their average total thickness in the Bełchatów deposit is in the range between 50–60 m and up to 240 m of the total thickness of the second Lusatian lignite seam (PGE Bełchatów). The total thickness of lignite in the Szczerców deposit varies from a few metres in the western part to ~40–70 m in the eastern part, including ~140 m in the upstream basin (Drobniak and Mastalerz, 2006).

RESULTS

Petrographic analysis of the lignite has used the following three lithotypes: detritic, detro-xylitic and xylitic. The samples from the Jóźwin (2B), Turów (4B) and Sieniawa (8B) deposits are xylitic lignite or xylite-rich lignite according to the ICCP classification. In the samples discussed, xylites represent at least 90% of the entire volume. Based on petrographic composition and the *GI* and *TPI* diagram (Fig. 3), it has been suggested that the lignite examined originated in a wet forest swamp environment. The sample collected from the Jóźwin (2B) deposit is characterized by the highest inertinite content among all samples analysed, reaching almost 20%, of which 14% is identified as fusinite.

The gelification of lignite is an important indicator of its potential applications, e.g. in the gasification process (Bielowicz, 2019). Gelification, determined by the presence of dark amorphous gels in lignite, can be assessed thanks to lithological description of coal and – more precisely – microscopic examination, allowing the distinguishing of macerals from the humocollinite subgroup, namely ulminite and densinite (Russell, 1984; Russell and Barron, 1984). The humocollinite subgroup belongs to a former maceral classification (ICCP, 1971). Fusinite originates from ligno-cellulosic cell walls. The botanical affinity of fusinite can be established when the cell structure is well-preserved ICCP, 2001a, b).It is suggested that the lignite seam examined from the Jóźwin deposit was affected by fire (Wang et al., 2019). A detritic lignite sample was collected from the Jóźwin deposit (1B). Detritic lignite, or lignite matrix according to the ICCP classification (Taylor et al., 1998), consists of fine humic particles (detritus) forming a more or less homogeneous macroscopic mass. As a lithotype, it contains up to 10% by volume of other components. The petrographic composition is dominated by macerals from the detrohuminite group, amounting to 83.5%. However, it should be noted that attrinite and densinite are accompanied by significant amounts of clay minerals and sand, locally up to 50%. Based on the *GI* and *TPI* indices, it is suggested that the detritic lignite sample examined was formed in an open marsh environment (Fig. 3).

Detro-xylitic coal and xylo-detritic lignite are both complex lithotypes, composed usually of xylites and humic detritus. Detro-xylitic coal is dominated by xylites, which should account by volume for more than half of the xylites and humic detritus

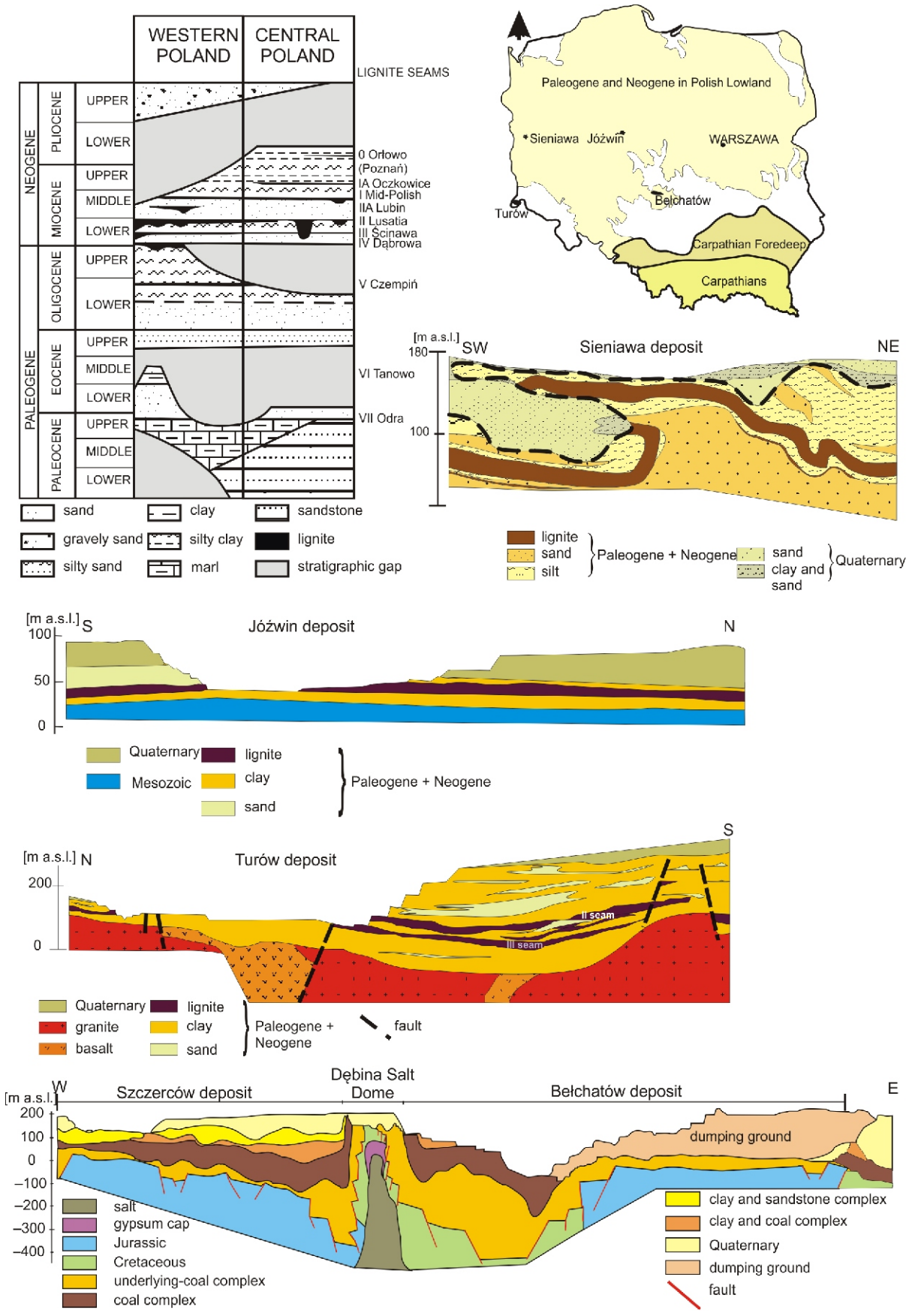

Fig. 2. Location of lignite deposits, Paleogene and Neogene stratigraphic columns in the Polish Lowland and geological cross-sections of lignite deposits in the surface mines examined (modified according to Czarnecki et al., 1992; Kozula, 1998, 2002; Kasiński et al., 2010; Bielowicz, 2012)

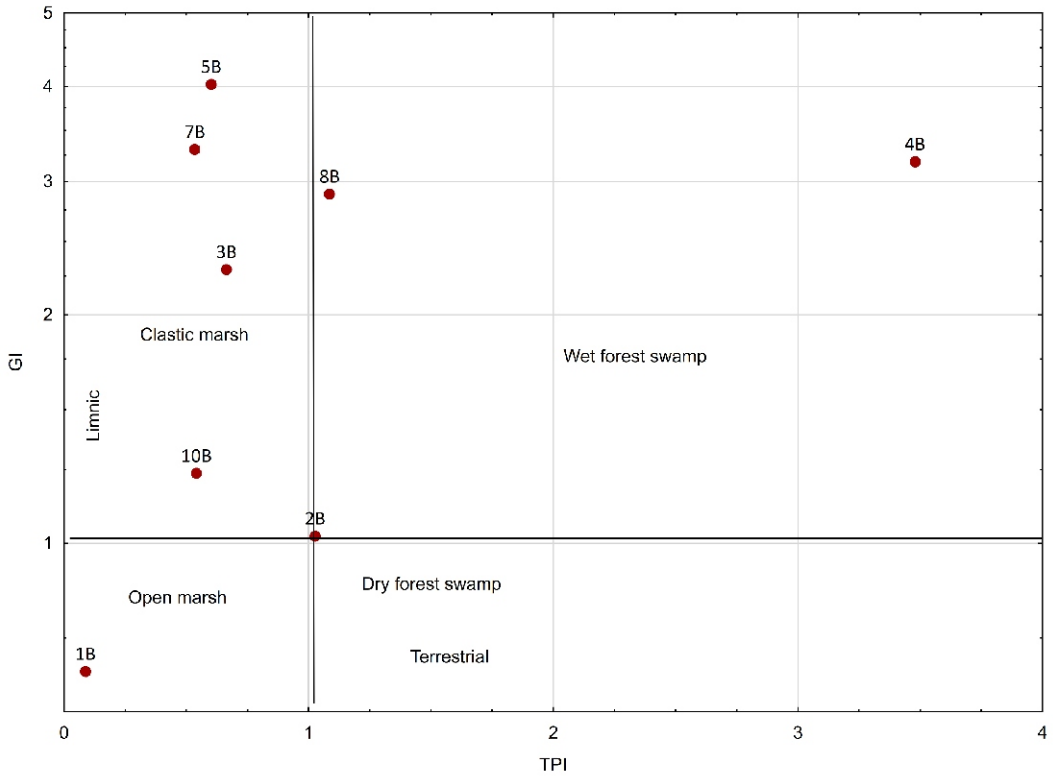

Fig. 3. The Gelification Index (*GI*) and Tissue Preservation Index (*TPI*) diagram, modified from Diessel (1986): 1B – Jóźwin detritic lignite; 2B – Jóźwin xylitic lignite; 3B – Jóźwin detro-xylitic lignite; 4B – Turów xylitic lignite; 5B – Turów xylo-detritic lignite; 7B – Sieniawa xylo-detritic lignite; 8B – Sieniawa xylitic lignite; 10B – Bełchatów xylo-detritic lignite

occurring in the specified layer (with at least 90% volume). Xylo-detritic lignite is dominated by humic detritus (Kwiecińska and Wagner, 1997, 2001). These lithotypes are represented by samples from the Jóźwin (3B), Turów (5B), Sieniawa (8B) and Bełchatów (10B) deposits.

The macerals from the telohuminite and detrohuminite subgroups dominate, in different proportions, in the samples examined (Table 2). It has been suggested that the lignite formed in a clastic marsh environment.

Generally, low proportions of macerals from the liptinite group were recorded in all of the lignite samples collected. The highest content (3.4%) was found for the xylo-detritic lignite from the Turów deposit. Macerals from the liptinite group found in the samples examined are mainly resinite, sporinite and cutinite. Macerals from the inertinite group are less commonly visible in the petrographic image. An inertinite content of up to 19.9% has been observed in only one sample (2B – Jóźwin xylitic).

In the samples examined of lignite, the ash content on a dry basis ranges from 2.3 wt.% (Table 3) in xylitic lignite from the Sieniawa deposit to 46.2 wt.% in detritic lignite from the Jóźwin deposit. The total sulphur content on a dry basis ranges from 0.53 wt.% in xylitic lignite from the Sieniawa deposit to 2.77 wt.% in detro-xylitic lignite from the Jóźwin deposit. The highest gross calorific value (daf), reaching up to 29.2 MJ/kg, is observed in the Turów deposit, while the lowest was in the Jóźwin deposit. Gross calorific value is associated with the rank of lignite. In the case of the samples analysed, the rank of lignite, the reflectance and the C^{daf} content is the highest in the Turów deposit. In general, according to the International Classification of In-Seam Coal (UN-ECE, 1998), all tested samples are classified as ortho lignite or low-rank C coal. The total porosity in the lignite examined ranges from 8.38% in xylo-detritic lignite from the Bełchatów deposit to 35.91% in xylo-detritic lignite from the Sieniawa deposit. The results obtained have shown that the lithotype composition has no effect on the porosity of the lignite.

The total porosity of up to 101.325 kPa can be explained by the presence of pores (cracks) with a diameter of ~7500 nm. The mercury pressure from 101.325 to 150 MPa corresponds to a pore range between 5 and 7500 nm. Thus, the difference between these values more or less corresponds to macro- and mesopores. Naturally, according to the IUPAC classification (Nič, 1997), the mesopore area is in the range of 50–2 nm, but excluding the 5–2 nm range does not seem to significantly affect the low value of porosity in the meso- and macropore area.

As for porosity, it can be observed that the samples examined are dominated by transport via pores and cracks. In the case of macro- and mesopores, that is, the areas where the sorption of gases and vapors takes place, the porosity is much lower. However, in the case of sorption phenomena, the volume of the pores, which was determined during sorption studies, is much more important than the porosity itself.

The results of linear adjustment of isotherms to experimental data are summarized in Table 4.

The table also includes the total pore volume *Vp*, surface area S_{BET} and the specific surface area of micropores S_{DR}.

The results of sorption analysis are summarized in Figure 4.

Table 2

Petrographic composition of the lignite

Sample		1B	2B	3B	4B	5B	7B	8B	10B
Deposit, lithotype		Jóźwin detritic	Jóźwin xylitic	Jóźwin detro-xylitic	Turów xylitic	Turów xylo-detritic	Sieniawa xylo-detritic	Sieniawa xylitic	Bełchatów xylo-detritic
Textinite	[vol %]	2.8	5.3	7.0	18.1	1.3	2.4	6.9	17.9
Ulminite	[vol %]	2.8	28.0	27.8	55.2	34.2	30.4	40.6	13.4
Telohuminite	[vol %]	5.6	33.3	34.8	73.2	35.5	32.9	47.5	31.3
Attrinite	[vol %]	49.9	21.6	17.5	4.2	16.8	18.9	16.5	21.3
Densinite	[vol %]	33.6	18.3	28.6	15.4	41.6	40.2	22.1	36.2
Detrohuminite	[vol %]	83.5	40.0	46.2	19.6	58.4	59.0	38.7	57.4
Corpohuminite	[vol %]	0.5	0.0	0.0	0.0	0.0	0.0	0.0	0.0
Gelinite	[vol %]	1.0	1.5	8.6	1.2	0.5	1.8	5.1	1.1
Gelohuminite	[vol %]	1.0	1.5	8.6	1.2	0.5	1.8	5.1	1.1
HUMINITE	[vol %]	90.6	74.8	89.6	94.0	94.5	93.7	91.3	89.9
Sporinite	[vol %]	0.5	0.3	1.0	0.3	0.7	0.6	0.2	0.3
Cutinite	[vol %]	0.2	0.1	0.1	0.1	0.3	0.1	0.0	0.2
Resinite	[vol %]	0.7	1.0	0.5	2.1	2.0	1.6	2.1	0.8
Suberinite	[vol %]	0.3	0.1	0.1	0.2	0.0	0.1	0.0	0.2
Alginite	[vol %]	0.1	0.0	0.1	0.0	0.0	0.0	0.0	0.1
Liptodetrinite	[vol %]	0.5	0.2	0.2	0.0	0.4	0.5	0.0	1.1
LIPTINITE	[vol %]	2.3	1.7	2.0	2.7	3.4	2.9	2.3	2.7
Fusinite	[vol %]	1.3	14.0	2.4	0.0	0.3	0.0	0.0	0.7
Semifusinite	[vol %]	0.8	0.0	0.0	0.0	0.0	0.0	0.0	0.4
Funginite	[vol %]	0.5	0.0	0.0	0.0	0.0	0.0	0.0	0.0
Micrinite	[vol %]	0.0	0.0	0.0	0.0	0.0	0.0	0.0	0.0
Inertodetrinite	[vol %]	0.0	4.7	1.3	0.3	0.5	0.6	0.0	0.7
INERTINITE	[vol %]	2.5	19.9	3.8	0.3	0.8	0.6	0.0	1.9
Pyrite	[vol %]	1.0	0.0	0.0	0.0	0.0	0.0	0.0	0.4
Carbonates	[vol %]	0.0	0.0	0.0	0.0	0.0	0.0	0.0	0.4
Quartz+Clays	[vol %]	3.6	3.6	4.6	3.0	1.3	2.7	6.4	4.8
MINERAL MATTER	[vol %]	4.6	3.6	4.6	3.0	1.3	2.7	6.4	5.6
The Gelification Index (*GI*)	–	0.7	1.0	2.3	3.2	4.0	3.3	2.9	1.2
The Tissue Preservation Index (*TPI*)	–	0.1	1.0	0.7	3.5	0.6	0.5	1.1	0.5
Random reflectance (R_o)	[vol %]	0.24	0.24	0.24	0.28	0.28	0.25	0.25	0.28

Table 3

Proximate and ultimate analysis of lignite samples

Sample		1B	2B	3B	4B	5B	7B	8B	10B
Deposit, lithotype		Jóźwin detritic	Jóźwin xylitic	Jóźwin detro-xylitic	Turów xylitic	Turów xylo-detritic	Sieniawa xylo-detritic	Sieniawa xylitic	Bełchatów xylo-detritic
Proximate analysis									
Moisture M^{ad}	[%]	7.6	8.2	9.6	8.4	10.0	10.5	7.6	9.8
Ash A^{ad}	[%]	42.7	5.7	22.2	4.6	3.4	6.2	2.1	14.6
Total sulphur S_t^{ad}	[%]	1.5	1.5	2.5	1.8	0.7	0.9	0.5	1.5
Gross calorific value GCV^{ad}	[MJ/kg]	11.9	22.3	17.8	25.2	25.3	21.9	22.4	19.4
Gross calorific value GCV^{daf}	[MJ/kg]	23.9	25.9	26.1	28.9	29.2	26.2	24.8	25.6
Net calorific value NCV^{ad}	[MJ/kg]	11.1	21.1	16.8	23.9	24.1	20.6	21.1	18.3
Total porosity (0–101.3 kPa) :	[%]	32.5	17.2	30.3	10.1	25.7	34.5	30.2	7.3
Total porosity (from 0.1 MPa to 150 MPa)	[%]	33.4	25.0	31.5	11.5	26.5	35.9	31.6	8.4
Macro +meso porosity	[%]	0.9	7.8	1.2	1.4	0.8	1.4	1.4	1.1
Ultimate analysis of lignite									
Carbon content C^{ad}	[%]	31.8	55.9	45.2	60.2	61.2	55.0	55.8	49.7
Hydrogen content H^{ad}	[%]	2.3	4.6	3.5	5.1	5.2	4.4	5.0	3.8
Carbon content C^{daf}	[%]	64.0	64.9	66.3	69.2	70.7	66.0	61.8	65.7
Hydrogen content H^{daf}	[%]	4.7	5.3	5.1	5.8	6.0	5.2	5.6	5.0
Fe	%	0.5	0.3	1.1	0.7	0.1	0.5	0.2	0.6
Ca	%	1.8	0.7	1.8	0.2	0.2	1.3	0.4	2.3
P	%	0.0	0.0	0.0	0.0	0.0	<0.00	0.0	0.0
Mg	%	0.4	0.1	0.4	0.2	0.2	0.1	0.0	0.1
Al	%	0.6	0.2	0.2	0.2	0.2	0.1	0.1	0.5
Na	%	0.0	0.0	0.0	0.3	0.3	0.0	0.0	0.0
K	%	0.0	<0.01	<0.01	0.0	0.0	<0.01	<0.01	0.0
Chemical composition of ash									
SiO_2	%	66.8	37.4	64.3	19.3	18.2	20.4	7.4	25.5
Al_2O_3	%	16.9	9.9	3.0	15.0	19.0	3.5	3.2	16.7
Fe_2O_3	%	2.2	7.8	6.3	21.9	6.2	11.7	17.6	7.2
MgO	%	1.6	3.5	2.3	6.4	11.0	2.4	2.1	2.2
CaO	%	6.1	18.1	9.4	4.9	8.4	26.1	30.0	23.6
Na_2O	%	0.1	0.3	0.1	7.8	12.3	0.3	0.1	0.5
K_2O	%	0.6	0.6	0.2	1.2	1.0	0.3	0.1	0.2
TiO_2	%	1.7	0.6	0.5	1.6	2.4	0.3	0.3	0.6
P_2O_5	%	0.0	0.3	0.0	0.2	0.2	0.0	0.0	0.2
MnO	%	0.1	0.1	0.2	0.0	0.0	0.1	0.2	0.2
Cr_2O_3	%	0.2	0.1	0.2	0.1	0.1	0.0	0.0	0.0
Other	%	3.8	21.2	13.6	21.5	21.2	34.9	38.9	23.1

ad – air dried content, daf – dry ash free content

Table 4

Comparison of isotherm constants

Parameter	Sample							
	1B	2B	3B	4B	5B	7B	8B	10B
	Jóźwin detritic	Jóźwin xylitic	Jóźwin detro-xylitic	Turów xylitic	Turów xylo-detritic	Sieniawa xylo-detritic	Sieniawa xylitic	Bełchatów xylo-detritic
Total pore volume V_p [cm^3/g]	0.186	0.026	0.144	0.088	0.231	0.395	0.243	0.014
The Langmuir isotherm equation								
$\frac{L}{m}$ [dm^3 STP /kg]	8.3	11.8	14.6	26.0	25.3	27.5	26.8	28.2
The DR isotherm equation								
W_0 [cm^3/g]	0.011	0.017	0.021	0.032	0.029	0.030	0.028	0.028
E_0 [kJ/mol]	23.6	24.3	25.2	26.0	24.7	21.2	21.7	20.3
S_{DR} [m^2/g]	0.1	0.1	0.1	0.2	0.2	0.2	0.1	0.1
The BET isotherm equation								
$\frac{BET}{m}$ [dm^3 STP/kg]	5.6	8.5	22.1	17.3	16.5	17.1	15.8	16.5
S_{BET} [m^2/g]	28.6	43.3	53.8	87.8	83.7	86.8	80.2	83.8

$\frac{L}{m}$, $\frac{BET}{m}$ – Langmuir and BET monolayer adsorption capacities; W_0 – the total micropore volume; E_0 – the characteristic energy of adsorption for a standard vapor; S_{DR}, S_{BET} – surface area determined using BET, DR equations

The experimental data were described using the Langmuir, BET and DR isotherms based on the calculated constants of the respective equations. The fitting of isotherms is very good for each sample, which indicates that all models accurately describe the coal-gas system. In the pressure range considered, the 4B and 1B samples were characterized by the highest and lowest CO_2 sorption capacity, respectively. Comparing the amounts obtained of the sorbed carbon dioxide to published data, this amount is either relatively high, slightly lower or comparable to the CO_2 sorption capacity of bituminous coal (Ozdemir et al., 2004; Dutka et al., 2013; Romanov et al., 2013; Zhang and Liu, 2017). In the case of bituminous coal, the sorption process takes place mainly in the area of micropores (Maphala and Wagner, 2012). When it comes to lignite, the low degree of metamorphism of the rock is the reason for lack of micropores in the structure and the presence of pores with larger diameters (Zhang and Liu, 2017). The DR equations for the samples examined, especially the value of S_{DR}, confirm that the lignites analysed are almost devoid of micropores. The results obtained of porosimetry studies in the field of high pressure (Table 3) support a low content of micropores. The low volume of W0 micropores and the calculated specific surface area of S_{DR} micropores indicate that the share of the smallest pores in relation to the total pore volume and specific surface area is small. The relatively high sorption capacity indicates that the sorption takes place in the mesopores. However, the sorption studies conducted do not allow direct measurement of the mesopores' distribution. Sorption capacity values are similar to those obtained for other Polish lignites (Baran et al., 2014), for which the absence of a microporous area were also found.

THE RELATIONSHIP BETWEEN PETROGRAPHIC COMPOSITION AND THE QUALITY AND SORPTION PROPERTIES OF LIGNITE

Analysis of the correlation between the petrographic compositions determined, proximate and ultimate analysis of lignite and the constants used in the Langmuir, DB and BET equations, was carried out. A clear relationship between sorption (Langmuir and DR) and ash content was observed (Fig. 5A).

The ash content increases with decreasing sorption. This is because the mineral matter, in particular quartz, a component of sands, has different sorption properties than lignite. A correlation between the chemical composition of ash and sorption capacity is clearly visible. The sorption capacity decreases with increasing SiO_2 content (Fig. 5B). The SiO_2 content in ash is mainly associated with quartz and clay minerals that occur in lignite. A very strong correlation between the coalification degree parameters expressed as NCV (Fig. 5C), C^{daf} and DR m^2/g, can be observed. Meanwhile, a relationship between Langumir DR, BET and mean random huminite reflectance is supported. The correlations marked in red in Table 5 should be considered as strong (Table 5).

There is also a very strong correlation between petrographic composition and sorption capacity. This relationship is particularly evident in the case of the Gelification Index and all constants of the sorption isotherm (Fig. 5D). A strongly negative correlation between attrinite and sorption capacity can also be observed (Table 5), although the porosity of attrinite should contribute to an increase in the sorption capacity. Attrinite may

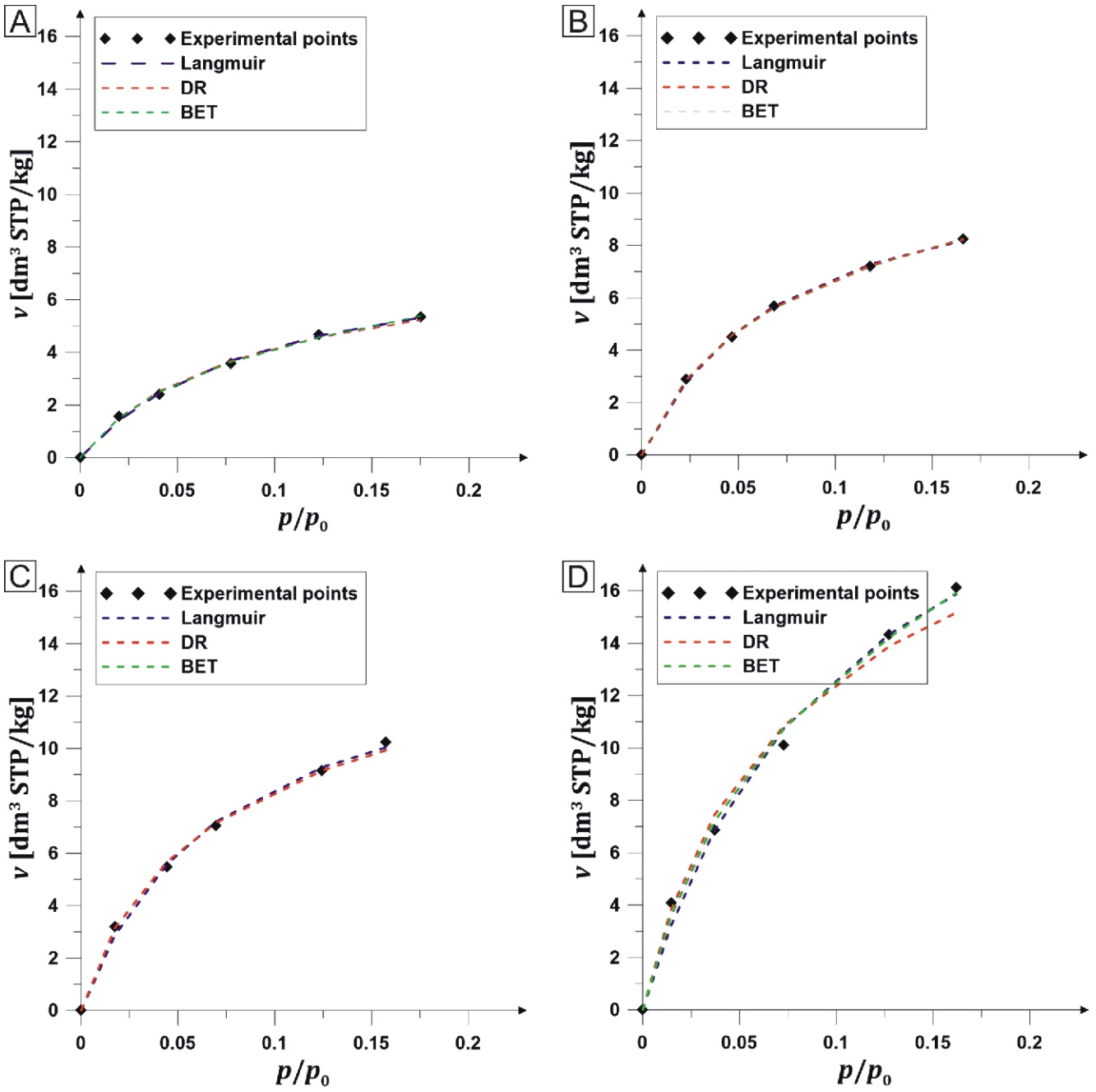

Fig. 4. Isotherms of CO_2 sorption for the following samples: A – 1B Jóźwin detritic lignite; B – 2B Jóźwin xylitic lignite; C – 3B Jóźwin detro-xylitic lignite; D – 4B Turów xylitic lignite; E – 5B Turów xylo-detritic lignite; F – 7B Sieniawa xylo-detritic lignite; G – 8B Sieniawa xylitic lignite; H – 10B Bełchatów xylo-detritic lignite

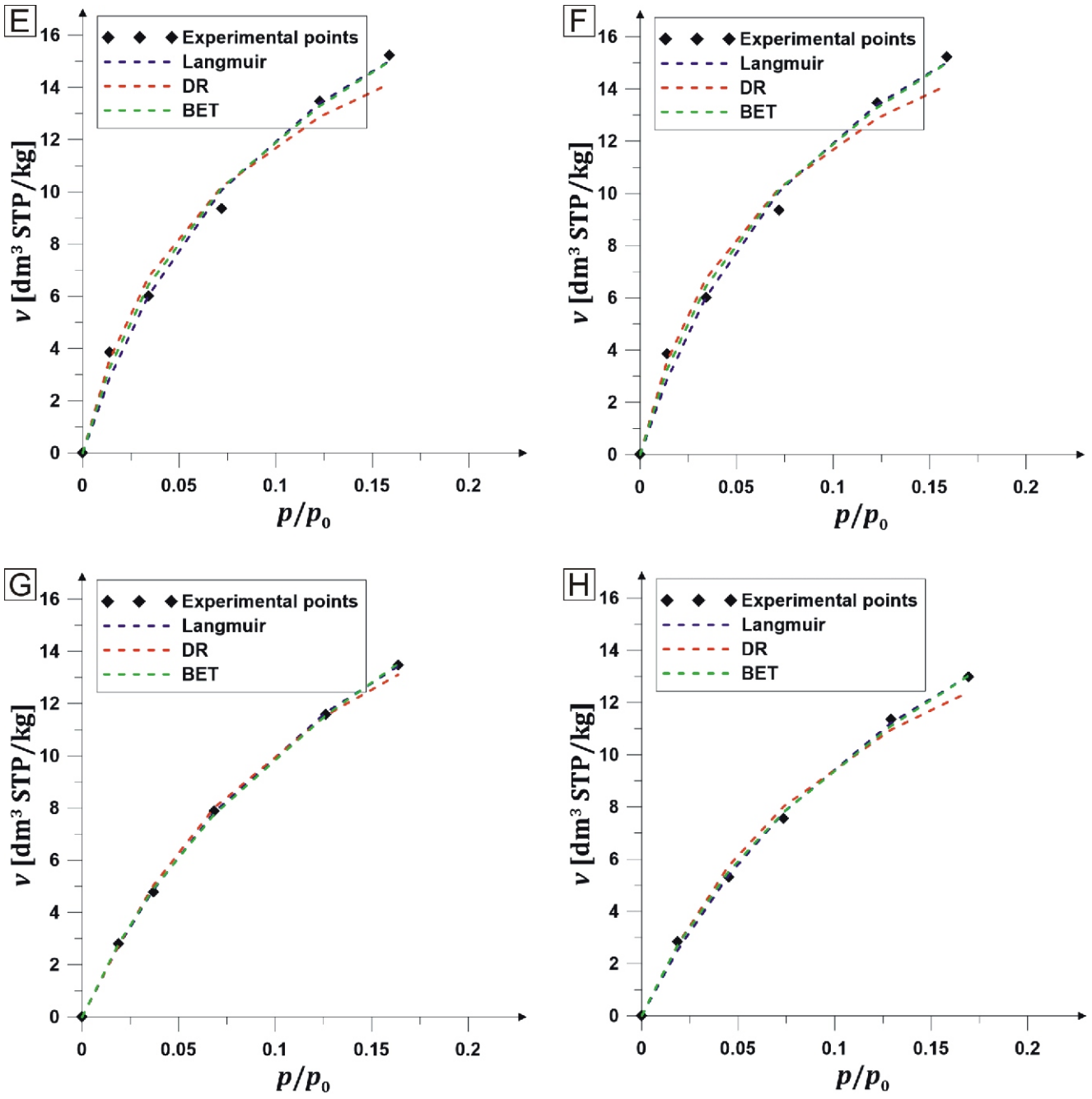

Fig. 4. cont.

contain finely dispersed mineral matter at sub-micron scale, invisible under the microscope, accompanying the lignitic matter and this mineral matter significantly inhibits sorption onto organic molecules. By contrast, the higher the content of telohuminite and liptinite in lignite, the more CO_2 is beings orbed. Moderately negative correlations between sorption capacity and inertinite were also observed.

The process of gelification starts during the peat stage, whereas at the stage of diagenesis this undergoes conversion into the vitrinites of subbituminous and bituminous coal (vitrinitization). The process involves a fragmentation of humic particles into a colloidal state and is paralleled by chemical transformations, manifested by an increase in carbon content in coal, a black colour and gloss. Gelification of humus can be considered taking into account physical, chemical or biochemical transformations of individual plant components, usually cellulose and lignin. In the light of current knowledge, it is the first stage of transformation (decomposition) of plant material, the product of which is known as humic gel (gelified coal) or organo-mineral gel (dopplerite; Wagner, 1982; Wagner et al., 1983). The transformations of plant aggregations, taking place at the peat stage, are referred to as humification or biochemical gelification (Stach and Murchison, 1982). This is one of the first stages during the gelification, i.e., the enrichment of the decomposing organic matter in carbon. It involves moderate oxidation and the development of so-called humic acids in the course of humification, peatification and putrefaction, which, in further stages of the process, are transformed into humines, i.e. chemical compounds without reactive functional groups. In the aquatic sedimentary environment, humic acids can react with inorganic bases or their salts. These reactions produce organic and mineral compounds including dopplerite (Wagner, 1982).

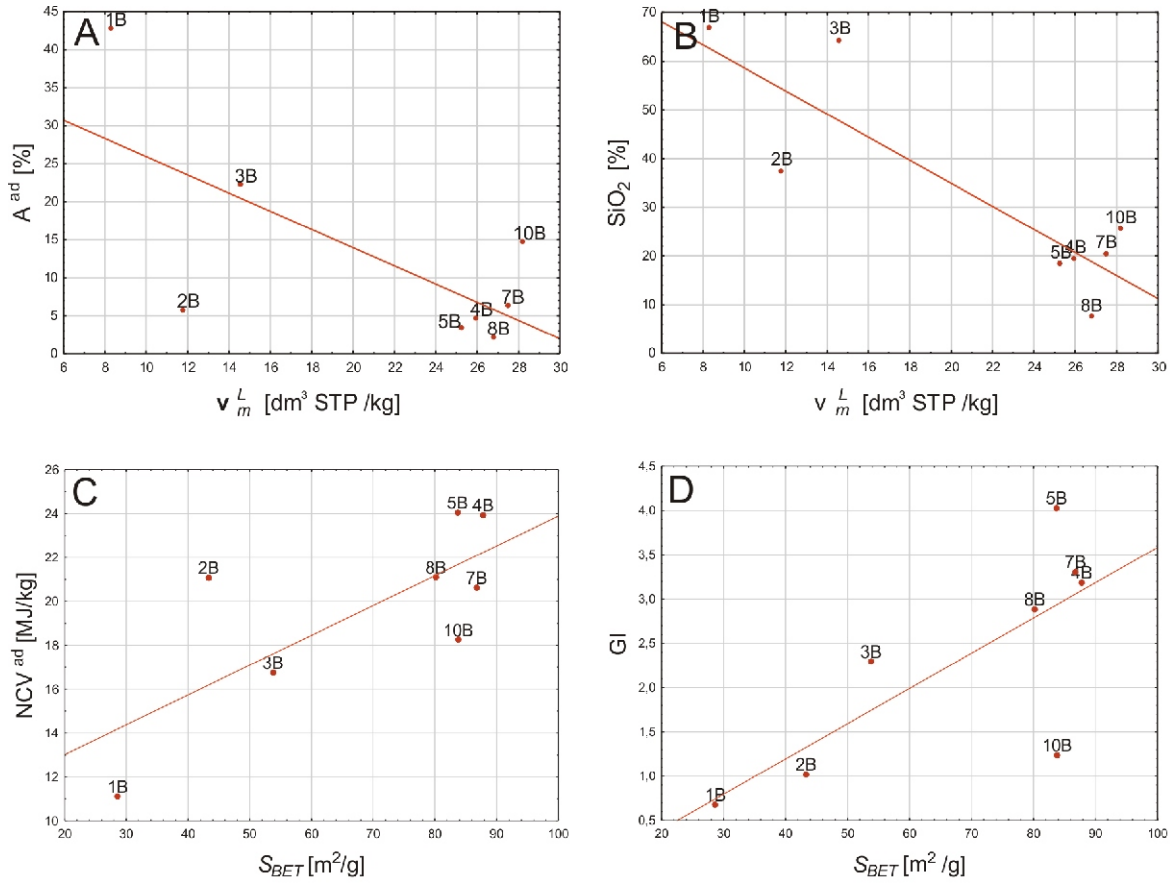

Fig. 5. The relationship between (A) ash in lignite and $\frac{L}{m}$; (B) SiO_2 in ash and $\frac{L}{m}$; (C) net calorific value and S_{BET}; (D) Gelification Index and $\frac{L}{m}$

A set of physical and chemical phenomena leading to the formation of such compounds can be called doppleritization (Wagner, 1982; Russell and Barron, 1984).

Gelified lignite significantly differs from ungelified varieties. Highly gelified varieties have a visibly conchoidal, uneven structure. Varieties of this type of coal are characterized by high brittleness, which is associated with a network of endogenous cracks.

Macroscopic features do not allow distinguishing humified coal from dopplerized coal. However, it is possible to distinguish both varieties based on the ash content, bound organically to carbon. Dopplerite coal is a mixture of Ca, K and Fe huminites. The ash content in coals with the highest degree of doppleritization is >10% by weight (Wagner et al., 1983). While the degree of gelification can be estimated macroscopically, its determination takes place by application of micro-petrographic analysis, e.g. the so-called Gelification Index (Diessel, 1986).The lignite samples examined were identified mainly as gelified coals. While no dopplerization has been observed, the Ca and Fe content in the detro-xylitic lignite sample from the Jóźwin deposit was higher (Ca – 1.8 ppm, Fe – 1.1 ppm) when compared to other coals examined and the ash content on a dry basis amounted to 24.6%. At the same time, this detro-xylitic lignite sample has a GI of 2.3 and a relatively low sorption capacity. Based on these results, it can be assumed that the increase in sorption capacity is affected only by the increase in the gelified matter content, while the content of dopplerized matter is irrelevant. The mesopores are formed in cracks (fissures) of the gelified lignite, where the majority of CO_2 sorption takes place. In the sample from the Bełchatów deposit, the low GI and a relatively high sorption capacity can be observed with a Ca content of 2.26%. A relatively high content of Ca is related to the presence of lacustrine chalk accompanying the humic matter (Wagner, 2007). It is suggested that the $CaCO_3$ content in lignite can increase its sorption capacity of CO_2.

The above analysis has shown that strongly gelified xylo-detritic and xylitic lignites with a high degree of coalification display the best sorption capacities. In the case of lignite, sorption is usually associated with mesopores (2–50 nm in diameter). The content of micropores (pores <2 nm in diameter) in the lignite examined is relatively low. The only exception is xylitic lignite with an inertinite content of 19.9% and micropore content of 7.75%. However, this micropore content has not led to an increase in the sorption capacity of lignite from the Jóźwin deposit. Generally, it can be concluded that lignite from this deposit has the lowest sorption capacity. This is related to the lowest rank of coal among all of the lignite seams examined.

CONCLUSION

The carbon dioxide sorption capacity of the lignites examined is highly variable despite their similar lithological development. The sorption isotherms determined were described using the Langmuir, BET and DR equations. The formal description of experimental isotherms allowed a determination of constant

Table 5

The correlation between sorption parameters and ultimate, proximate and petrographic analysis (in red – the correlation is statistically significant, with statistical significance = 0.1)

	$\frac{L}{m}$ [dm^3 STP /kg]	W_0 [cm^3/g]	S_{DR} [m^2/g]	$\frac{BET}{m}$ [dm^3 STP/kg]	S_{BET} [m^2/g]
M^{ad} [%]	0.46	0.49	0.49	0.61	0.51
A^{ad} [%]	–0.70	–0.77	–0.47	–0.43	–0.74
S_t^{ad} [%]	–0.49	–0.36	–0.30	0.19	–0.42
GCV^{ad} [MJ/kg]	0.66	0.79	0.63	0.44	0.74
GCV^{daf}[MJ/kg]	0.45	0.63	0.80	0.46	0.58
NCV^{ad} [MJ/kg]	0.66	0.78	0.63	0.43	0.74
C^{ad} [%]	0.68	0.79	0.60	0.43	0.75
H^{ad} [%]	0.64	0.74	0.54	0.38	0.70
C^{daf} [%]	0.28	0.44	0.75	0.37	0.40
H^{daf} [%]	0.51	0.66	0.63	0.38	0.61
Total porosity [%] (from 101,3 kPa)	–0.27	–0.30	0.00	–0.05	–0.29
Total porosity [%] (from 150 kPa)	–0.38	–0.39	–0.07	–0.15	–0.39
High-pressure porosity [%]	–0.43	–0.37	–0.28	–0.46	–0.40
Textinite [%]	0.39	0.40	–0.06	0.30	0.39
Ulminite [%]	0.52	0.70	0.57	0.51	0.62
Telohuminite [%]	0.58	0.74	0.46	0.54	0.66
Attrinite [%]	–0.67	–0.83	–0.48	–0.74	–0.76
Densinite [%]	0.20	0.07	0.24	0.11	0.16
Detrohuminite [%]	–0.35	–0.53	–0.20	–0.45	–0.44
Corpohuminite [%]	–0.64	–0.74	–0.29	–0.71	–0.70
Gelinite [%]	–0.16	–0.09	–0.42	0.54	–0.14
Gelohuminite [%]	–0.16	–0.09	–0.42	0.54	–0.14
HUMINITE [%]	0.57	0.55	0.56	0.49	0.57
LIPTINITE [%]	0.69	0.67	0.79	0.32	0.71
INERTINITE [%]	–0.58	–0.53	–0.39	–0.48	–0.56
Pyrite [%]	–0.50	–0.66	–0.39	–0.66	–0.59
Quartz+Clays [%]	0.01	–0.11	–0.76	0.09	–0.10
Mineral matter [%]	–0.07	–0.23	–0.82	–0.05	–0.19
GI	0.67	0.79	0.79	0.64	0.75
TPI	0.31	0.48	0.42	0.25	0.40
R_o [%]	0.72	0.72	0.54	0.36	0.74
Fe [%]	–0.25	–0.14	–0.16	0.44	–0.19
Ca [%]	–0.26	–0.40	–0.53	–0.02	–0.34
P [%]	0.06	–0.07	–0.45	–0.14	–0.01
Mg [%]	–0.65	–0.59	–0.21	–0.08	–0.61
Al [%]	–0.38	–0.53	–0.46	–0.43	–0.46
Na [%]	0.37	0.50	0.72	0.25	0.47
K [%]	–0.48	–0.52	0.03	–0.61	–0.50
Ash composition					
SiO_2 [%]	–0.87	–0.83	–0.49	–0.29	–0.85
Al_2O_3 [%]	–0.03	–0.07	0.19	–0.38	–0.03
Fe_2O_3 [%]	0.59	0.68	0.40	0.36	0.63
MgO [%]	0.30	0.42	0.68	0.19	0.40
CaO [%]	0.47	0.30	–0.23	0.11	0.36
Na_2O [%]	0.34	0.47	0.72	0.21	0.44
K_2O [%]	0.01	0.16	0.63	–0.17	0.12
TiO_2 [%]	–0.09	–0.02	0.47	–0.21	–0.02
P_2O_5 [%]	–0.01	0.04	0.03	–0.24	0.03
MnO [%]	–0.07	–0.21	–0.73	0.02	–0.18
Cr_2O_3 [%]	–0.93	–0.85	–0.34	–0.42	–0.89

equations of sorption isotherms. It has been shown that all the three equations describe well the coal-gas system examined. The analysis of the constants of the DR equation has shown that the lignite samples analysed contain practically no micropores, hence the mesopore pores are the reason behind their relatively high sorption capacity. The calculated constants were subjected to statistical analysis in relation to the parameters obtained as a result of elemental, technological and petrographic analysis. It has been found that the CO_2 sorption capacity is clearly associated with the Gelification Index. The degree of gelification of macerals from the huminite group is indicated by the Gelification Index (*GI*), which differentiates gelified macerals from ungelified ones. A continuous presence of water is a prerequisite for gelification, while fluctuation in the water table affects the *GI*; this is due to the fact that inertinites are usually formed during dry periods. Therefore, it can be concluded that the sorption properties increase with an increasing content of gelified components. In the case of the samples examined, the lowest sorption capacity has been recorded for detritic lignite with a high ash content, which, at the same time, displayed the lowest rank. The CO_2 sorption capacity of coal increases with the degree of coalification and is the highest in mixed detro–xylitic and xylo-detritic lithotypes with low attrinite content. Based on the results obtained, a preliminary determination of the sorption properties of the prospective deposits can be made and the suitability of coal for CO_2 storage can be assessed.

Acknowledgements. This article was supported by the Polish National Science Centre through a research project awarded by decision No. DEC-2013/09/D/ST10/04045. The authors would like to thank Dr. A. Pajdak and the anonymous reviewer for insightful reviews.

REFERENCES

Azmi, AS., Yusup, S., Muhamad, S., 2006. The influence of temperature on adsorption capacity of Malaysian coal. Chemical Engineering and Processing: Process Intensification, **45**: 392–396.

Baran, P., Zarębska, K., 2015. Estimating the limiting absolute sorption of carbon dioxide by coal for coal-bed storage of carbon dioxide. International Journal of Oil, Gas and Coal Technology, **10**: 179–193.

Baran, P., Broś, M., Nodzeński, A., 2010. Studies on CO_2 sorption on hard coal in the near-critical area with regard to the aspect of sequestration. Archiwum Górnictwa, **55**: 59–68.

Baran, P., Cygankiewicz, J., Zarębska, K., 2013. Carbon dioxide sorption on Polish ortholignite coal in low and elevated pressure. Journal of CO_2 Utilization, **3–4**: 44-48.

Baran, P., Zarębska, K., Nodzeński, A., 2014. Energy aspects of CO_2 sorption in the context of sequestration in coal deposits. Journal of Earth Science, **25**: 719–726.

Bielowicz, B., 2012. A new technological classification of low-rank coal on the basis of Polish deposits. Fuel, **96**: 497–510.

Bielowicz, B., 2019. The suitability of Polish lignite for gasification. Clean Technologies and Environmental Policy, **21**: 1115–1130.

Bielowicz, B., Kasiński, J.R., 2014. The possibility of underground gasification of lignite from Polish deposits. International Journal of Coal Geology, **131**: 304–318.

Botnen, L.S., Fisher, D.W., Dobroskok, A.A., Bratton, T.R.H., Greaves, K., McLendon, T., Steiner, G., Sorensen, J.A., Steadman, E.N., Harju, J.A., 2009. Field test of CO_2 injection and storage in lignite coal seam in North Dakota. Energy Procedia, **1**: 2013–2019.

Brunauer, S., Emmett, P.H., Teller, E., 1938. Adsorption of gases in multimolecular layers. Journal of the American Chemical Society, **60**: 309–319.

Clarkson, C.R., Bustin, R.M., 1997. Variation in permeability with lithotype and maceral composition of Cretaceous coals of the Canadian Cordillera. International Journal of Coal Geology, **33**: 135–151.

Crosdale, P.J., Beamish, B.B., Valix, M., 1998. Coalbed methane sorption related to coal composition. International Journal of Coal Geology, **35**: 147–158.

Czarnecki L., Frankowski R., Ślusarczyk G., 1992. Syntetyczny profil litostratygraficzny rejonu złoża Bełchatów dla potrzeb Bazy Danych Geologicznych (in Polish). Górnictwo Odkrywkowe, **3–4**.

Diessel, C.F.., 1986. On the correlation between coal facies and depositional environments. In: Proceedings of the 20th Symposium on Advances in the Study of the Sydney Basin, Deparment of Geology, University of Newcastle: 19–22.

Drobniak, A., Mastalerz, M., 2006. Chemical evolution of Miocene wood: example from the Belchatow brown coal deposit, central Poland. International Journal of Coal Geology, 66: 157–178.

Dubinin, M.M., 1960. The potential theory of adsorption of gases and vapors for adsorbents with energetically nonuniform surfaces. Chemical Reviews, **60**: 235–241.

Dutka, B., Kudasik, M., Pokryszka, Z., Skoczylas, N., Topolnicki, J., Wierzbicki, M., 2013. Balance of CO_2/CH_4 exchange sorption in a coal briquette. Fuel Processing Technology, **106**: 95–101.

Gale, J., Freund, P., 2001. Coal-bed methane enhancement with CO_2 sequestration worldwide potential. Environmental Geosciences, **8**: 210–217.

Gensterblum, Y., van Hemert, P., Billemont, P., Battistutta, E., Busch, A., Krooss, B.M., De Weireld, G., Wolf, K.-H.A.A., 2010. European inter-laboratory comparison of high pressure CO_2 sorption isotherms II: natural coals. International Journal of Coal Geology, **84**: 115–124.

Grimes, W.R., 1982. The Physical Structure of Coal: 21–42. Academic Press.

Harpalani, S., Mitra, A., 2010. Impact of CO_2 injection on flow behavior of coalbed methane reservoirs. Transport in Porous Media, **82**: 141–156.

ICCP, 1971. International Handbook of Coal Petrography, 1st Supplement to 2nd Edition. CNRS, Paris.

ICCP, 2001a. The new inertinite classification (ICCP System 1994). Fuel, **80**: 459–471.

ICCP, 2001b. The new vitrinite classification (ICCP System, 1994). Fuel, **80**: 459–471.

ISO 13909-1:2016. Hard coal and coke – Mechanical sampling.

ISO 7404-2:2009. Methods for the petrographic analysis of coals – Part 2: Methods of preparing coal samples. Methods for the petrographic analysis of coals – Part 3: Method of determining maceral group composition.

Kalaitzidis, S., Bouzinos, A., Papazisimou, S., Christanis, K., 2004. A short-term establishment of forest fen habitat during Pliocene lignite formation in the Ptolemais Basin, NW Macedonia, Greece. International Journal of Coal Geology, **57**: 243–263.

Karczewska, A., Chodak, T., Kaszubkiewicz, J., 1996. The suitability of brown coal as a sorbent for heavy metals in polluted soils. Applied Geochemistry, **11**: 343–346.

Kasiński, J.., Piwocki, M., Sadowska, E., Ziembińska-Tworzydło, M., 2010. Lignite of the Polish Lowlands Miocene: characteristics on a base of selected profiles (in Polish with English summary). Biuletyn Państwowego Instytutu Geologicznego, **439**: 99–154.

Kozula, R., 1998. Dodatek nr 1 do dokumentacji eologicznej w kategorii B złoża węgla brunatnego Pątnów IV w Kleczewie (in Polish). Archiwum KWB Konin.

Kozula, R., 2002. Dokumentacja geologiczna złoża węgla brunatnego „Sieniawa" w kategorii C1 (in Polish). Archiwum KWB Sieniawa S.A.

Kudasik, M., Skoczylas, N., Pajdak, A., 2017. The repeatability of sorption processes occurring in the coal-methane system during multiple measurement series. Energies, **10**.

Kwiecińska, B., Wagner, M., 1997. Typizacja cech jakościowych węgla brunatnego z krajowych złóż według kryteriów petrograficznych i chemiczno-technologicznych do celów dokumentacji geologicznej złóż oraz obsługi kopalń (in Polish). Wydawnictwo Centrum PPGSMiE PAN, Kraków.

Kwiecińska, B., Wagner, M., 2001. Atlas petrograficzny węgla brunatnego – litotypy i macerały (in Polish). Wydawnictwo JAK Andrzej Choczewski, Kraków.

Lamberson, M.N., Bustin, R.M., Kalkreuth, W., 1991. Lithotype (maceral) composition and variation as correlated with paleo-wetland environments, Gates Formation, northeastern British Columbia, Canada. International Journal of Coal Geology, **18**: 87–124.

Langmuir, I., 1918. The adsorption of gases on plane surfaces of glass, mica and plutonium. Journal of the American Chemical Society, **40**: 1361–1403.

Laxminarayana, C., Crosdale, P.J., 1999. Role of coal type and rank on methane sorption characteristics of Bowen Basin, Australia coals. International Journal of Coal Geology, **40**: 309–325.

Li, X., Fang, Z., 2014. Current status and technical challenges of CO_2 storage in coal seams and enhanced coalbed methane recovery: an overview. International Journal of Coal Science and Technology, **1**: 93–102.

Macuda, J., Nodzeński, A., Wagner, M., Zawisza, L., 2011. Sorption of methane on lignite from Polish deposits. International Journal of Coal Geology, **87**: 41–48.

Maphala, T., Wagner, N.J., 2012. Effects of CO_2 storage in coal on coal properties, 6th Trondheim Carbon Capture and Storage Conference (TCCS-6). Energy Procedia, **23**: 426–438.

Mastalerz, M., Gluskoter, H., Rupp, J., 2004. Carbon dioxide and methane sorption in high volatile bituminous coals from Indiana, USA. International Journal of Coal Geology, **60**: 43–55.

Mazzotti, M., Pini, R., Storti, G., 2009. Enhanced coalbed methane recovery. The Journal of Supercritical Fluids, **47**: 619–627.

Nič, M., 1997. IUPAC Compendium of Chemical Terminology 2nd Edition. IUPAC Compendium of Chemical Terminology Gold Book 2.

Ozdemir, E., Morsi, B.I., Schroeder, K., 2004. CO_2 adsorption capacity of argonne premium coals. Fuel, **83**: 1085–1094.

Pan, Z., Ye, J., Zhou, F., Tan, Y., Connell, L.D., Fan, J., 2018. CO_2 storage in coal to enhance coalbed methane recovery: a review of field experiments in China. International Geology Review, **60**: 754–776.

Perera, M.S.A., Ranjith, P.G., 2015. Enhanced Coal Bed Methane Recovery: Using Injection of Nitrogen and Carbon Dioxide Mixture. Handbook of Clean Energy Systems. John Wiley & Sons.

PGI-NRI, 2017. PGI-NRI [WWW Document]. http://geoportal.pgi.gov.pl/surowce

Pickel, W., Kus, J., Flores, D., Kalaitzidis, S., Christanis, K., Cardott, B.J., Misz-Kennan, M., Rodrigues, S., Hentschel, A., Hamor-Vido, M., Crosdale, P., Wagner, N., 2017. Classification of liptinite – ICCP System 1994. International Journal of Coal Geology, **169**: 40–61.

Piwocki, M., 2004. Paleogen (in Polish). In: Budowa Geologiczna Polski, **1**: Stratygrafia. Part 3a: Kenozoik, Paleogen, Neogen (eds. T.M. Peryt and M. Piwocki): 22–71. Państwowy Instytut Geologiczny.

Piwocki, M., Ziembińska-Tworzydło, M., 1997. Neogene of the Polish Lowlands – lithostratigraphy and pollen-spore zones. Geological Quarterly, **41** (1): 21–40.

Reznik, A.A., Singh, P.K., Foley, W.L., 1984. An analysis of the effect of CO_2 injection on the recovery of in-situ methane from bituminous coal: an experimental simulation. Society of Petroleum Engineers Journal, **24**: 521–528.

Romanov, V.N., Hur, T.B., Fazio, J.J., Howard, B.H., Irdi, G.A., 2013. Comparison of high-pressure CO_2 sorption isotherms on Central Appalachian and San Juan Basin coals. International Journal of Coal Geology, **118**: 89–94.

Russell, N.J., 1984. Gelification of Victorian tertiary soft brown coal wood. I. Relationship between chemical composition and microscopic appearance and variation in the degree of gelification. International Journal of Coal Geology, **4**: 99–118.

Russell, N.J., Barron, P.F., 1984. Gelification of Victorian tertiary soft brown coal wood. II. Changes in chemical structure associated with variation in the degree of gelification. International Journal of Coal Geology, **4**: 119–142.

Sadowska, A., Giża, B., 1991. The flora and age of the brown coal from Pątnów. Acta Palaeobotanica, **31**: 215–225.

Span, R., Wagner, W., 1996. A new equation of state for carbon dioxide covering the fluid region from the triple-point temperature to 1100 k at pressures up to 800 MPa. Journal of Physical and Chemical Reference Data, **25**: 1509–1596.

Stach, E., Murchison, D., 1982. Stach's Textbook of coal Petrology. Borntraeger, Berlin.

Švábová, M., Weishauptová, Z., Přibyl, O., 2012. The effect of moisture on the sorption process of CO_2 on coal. Fuel, **92**: 187–196.

Sýkorová, I., Pickel, W., Christanis, K., Wolf, M., Taylor, G.H., Flores, D., 2005. Classification of huminite – ICCP System 1994. International Journal of Coal Geology, **62**: 85–106.

Szwed-Lorenz, J., 1991. Petrologic evaluation of Polish soft brown coals as raw material for different use. Prace Naukowe Instytutu Górnictwa Politechniki Wrocławskiej, **63**, Monogr., 29. Wrocław.

Taylor, G.H., Teichmuller, M., Davis, A., Diessel, C.F.K., Littke, R., Robert, P., 1998. Organic Petrology: A New Handbook Incorporating Some Revised Parts of Stach's Textbook of Coal Petrology. Gebrüder Borntraeger, Berlin.

UN-ECE, 1998. International Classification of In-Seam Coals Symbol Number: ENERGY/1998/19 [WWW Document].

Wagner, M., 1982. Doppleritization of xylitic coal in the light of petrographic and chemical investigations. International Journal of Coal Geology, **2**: 181–194.

Wagner, M., 2007. Zmienność petrologiczno-sedymentologiczna i własności technologiczne kredy jeziornej w osadach neogenu typu wapiennego zapadliska tektonicznego na przykładzie złoża węgla brunatnego „Szczerców" (in Polish). AGH Uczelniane Wydawnictwa Naukowo-Dydaktyczne, Kraków.

Wagner, M., Żerda, T., John, A., 1983. Gelification in the light of petrographic and physico-chemical studies (in Polish with English summary). Geological Quarterly, **27** (1): 87–104.

Wang, K., Fu, X., Qin, Y., Sesay, S.K., 2011. Adsorption characteristics of lignite in China. Journal of Earth Science, **22**: 371–376.

Wang, S., Shao, L.-Y., Yan, Z.-M., Shi, M.-J., Zhang, Y.-H., 2019. Characteristics of Early Cretaceous wildfires in peat-forming environment, NE China. Journal of Palaeogeography, **8**: 17.

Zelenka, T., Taraba, B., 2014. Sorption of CO_2 on low-rank coal: Study of influence of various drying methods on microporous characteristics. International Journal of Coal Geology, **132**: 1–5.

Zhang, R., Liu, S., 2017. Experimental and theoretical characterization of methane and CO_2 sorption hysteresis in coals based on Langmuir desorption. International Journal of Coal Geology, **171**: 49–60.